Heliyon 6 (2020) e05877

Contents lists available at ScienceDirect

Heliyon

journal homepage: www.cell.com/heliyon

Research article

Clinically distinct COVID-19 cases share notably similar immune response progression: A follow-up analysis

Melissa A. Hausburg [a,b,c,d], Kaysie L. Banton [a], Michael Roshon [d], David Bar-Or [a,b,c,d,e,*]

[a] Trauma Research Department, Swedish Medical Center, Englewood, CO, USA
[b] Trauma Research Department, St. Anthony Hospital, Lakewood, CO, USA
[c] Trauma Research Department, Penrose Hospital, Colorado Springs, CO, USA
[d] Emergency Room Department, Penrose Hospital, Colorado Springs, CO, USA
[e] Department of Molecular Biology, Rocky Vista University, Parker, CO, USA

ARTICLE INFO

Keywords:
SARS-CoV-2
COVID-19
SERPING1
Complement
B cell
Interferon
MHC class II

ABSTRACT

Inflammatory responses to the novel coronavirus SARS-CoV-2, which causes COVID-19, range from asymptomatic to severe. Here we present a follow-up analysis of a longitudinal study characterizing COVID-19 immune responses from a father and son with distinctly different clinical courses. The father required a lengthy hospital stay for severe symptoms, whereas his son had mild symptoms and no fever yet tested positive for SARS-CoV-2 for 29 days. Father and son, as well as another unrelated COVID-19 patient, displayed a robust increase of SERPING1, the transcript encoding C1 esterase inhibitor (C1–INH). We further bolstered this finding by incorporating a serum proteomics dataset and found that serum C1–INH was consistently increased in COVID-19 patients. C1–INH is a central regulator of the contact and complement systems, potentially linking COVID-19 to complement hyperactivation, fibrin clot formation, and immune depression. Furthermore, despite distinct clinical cases, significant parallels were observed in transcripts involved in interferon and B cell signaling. As symptoms were resolving, widespread decreases were seen in immune-related transcripts to levels below those of healthy controls. Our study provides insight into the immune responses of likely millions of people with extremely mild symptoms who may not be aware of their infection with SARS-CoV-2 and implies a potential for long-lasting consequences that could contribute to reinfection risk.

1. Introduction

Coronavirus disease 2019 (COVID-19), which is caused by infection with the novel coronavirus SARS-Coronavirus-2 (SARS-CoV-2), was first described in Wuhan, China, at the end of 2019. COVID-19 and SARS-CoV-2 infections rapidly spread, and COVID-19 was declared a pandemic by the World Health Organization in March of 2020.

The response to the COVID-19 pandemic by the scientific community has resulted in a concentrated effort of historical proportions, including widespread data sharing in the hopes of understanding every aspect of SARS-CoV-2 and COVID-19. Symptoms of SARS-CoV-2 infection are varied, as some patients are asymptomatic, whereas others suffer from cough, dyspnea, respiratory failure, cytokine storm, and, in many cases, death [1]. Furthermore, our understanding of COVID-19 symptoms continues to evolve as unexpected consequences of SARS-CoV-2 infection come to light, e.g., potential increased risk of thrombotic events in COVID-19 patients [2, 3, 4, 5, 6]. SARS-CoV-2 infections spread through contact with symptomatic, as well as pre-symptomatic and asymptomatic, cases [7]. A detailed characterization of immune responses to SARS-CoV-2 infection in pre-symptomatic, mild, and asymptomatic cases is warranted and imperative for the identification of predictive biomarkers and effective vaccination programs.

Our goal was to apply statistical comparisons to the three clinical case subjects from Wuhan, China, presented by Ong et al., as the original paper was not subjected to statistical analysis [8]. These data are unique because cases 1 and 2 are father and son with starkly different clinical courses of COVID-19 infection. These two cases represent a dataset with reduced genetic diversity and offer the ability to compare a severe to a mild case temporally, as Ong et al. characterized whole blood mRNA ranging from early in the clinical course to as late as 19 days from symptom onset (DSO) [8].

* Corresponding author.
E-mail address: davidbme49@gmail.com (D. Bar-Or).

https://doi.org/10.1016/j.heliyon.2020.e05877
Received 9 June 2020; Received in revised form 12 August 2020; Accepted 24 December 2020

Case 1, a 66-year-old male, presented with fever (38.1 °C), cough, and, as defined by Ong et al., "bilateral, patchy, ill-defined lung infiltrates" [8]. For the purposes of our study, we classified case 1 as a severe COVID-19 case, consistent with previous studies [9]. At 5 DSO, when his arterial O_2 saturation (SO_2) reached a nadir despite 4 L of supplemental oxygen, case 1 received the anti-viral medication lopinavir-ritonavir; however, anti-viral administration did not prevent case 1 from testing positive for SARS-CoV-2 at 7, 12, and 18 DSO. Case 1 was deemed fit for discharge on 22 DSO.

The son of case 1 was case 2, a 37-year-old who began to have COVID-19 symptoms just prior to the onset of symptoms in case 1. Case 2 reported having a single day of diarrhea and, two days later, a cough and mild sore throat. Ong et al. deemed day 1 of his clinical course as the day that the sore throat and cough symptoms began [8]. The concept of DSO is subjective and, in cases 1 and 2, symptom onset was so closely reported that it is likely that father and son became inoculated with SARS-CoV-2 at, or closely around, the same time. The son self-reported a mild sore throat and cough on January 19, and the father self-reported a fever on January 20 [8]. A fever is a quantitative measurement and indicates a systemic inflammatory response, and this was set as 1 DSO, in the case of the father. Complicating the situation, the son never reported or developed a fever. Assignment of 1 DSO was set at the time the son developed a mild sore throat and cough, one day prior to the father's reported fever. The overall timing and relationship of father and son suggests these samples were closely matched in time of infection, regardless of the DSO reported in Ong et al. [8]. Case 2's cough persisted until 19 DSO, yet he tested positive for SARS-CoV-2 during 1–21 DSO and again on 23, 26, and 29 DSO, the latter being a full 10 days after symptom resolution. For these analyses, case 2 was deemed to be a mild case, as he was afebrile and never required medical support.

Case 3 was an unrelated 37-year-old man that presented to the hospital with fever, non-productive cough, lethargy, and myalgia and was confirmed positive for SARS-CoV-2 on 7 DSO. Throat swabs from case 3 tested positive for SARS-CoV-2 consistently until 17 DSO and intermittently until 23 DSO. We deemed his case to be moderate as he did not require any supplemental oxygen.

In a related study, Hadjadi et al. characterized whole blood mRNA from 32 COVID-19 patients separated into groups by disease severity, mild/moderate, severe, and critical [10], and herein we provide comparisons to these data. We also compare our findings to those of Shen et al. that performed a full proteomics and metabolomic analysis of COVID-19 patient serum [11].

By applying unbiased sample grouping and statistical methods, this dataset may provide a window into the temporal dynamics of COVID-19-related immune responses in afebrile patients with mild symptoms.

2. Methods

2.1. Hierarchical clustering and PCA analysis

Data were generated by Ong et al. using the Human Immunology V2 multiplex panel available from NanoString Technologies, Inc [8]. Raw data were obtained from Array Express, accession number E-MTAB-8871, and uploaded into the nSolver Analysis software (NanoString Technologies, Inc.) for further analysis. All data, analysis software, and patient information used in this study are freely available to the public. These data were not generated from patients at any of our facilities, and thus, institutional review board oversight was not necessary, and the analysis of secondary, de-identified, publicly available data does not constitute research involving human subjects under the federal Common Rule, 45 CFR Part 46. Only case 1 day 4 was run in technical duplicates, and as no other sample was run in replicate, we removed the second replicate for this sample from any further analysis. Data were subjected to the Advanced Analysis Module of the nSolver software and were normalized using default settings (Figure 1). For heatmap generation, each line represents a single gene, each column is a separate sample, and means were scaled (z-score) to give all genes equal variance. The clustering dendrogram was generated unsupervised using Euclidean distance and complete linkage. Orange corresponds to higher expression, and blue corresponds to lower expression. Principal component analysis (PCA) plots were auto generated by nSolver Advanced Analysis software, NanoString, Technologies Inc.

2.2. Pathway analysis

nSolver software condensed each covariate's gene expression profiles into pathway scores. Pathway scores were fit using the first principal component of the data for each gene set. A positive score indicates that at least half of the genes in that pathway's set have positive weights, and vice versa for negative scores. Pathway scores were subjected to gaussian statistical analysis t-tests with homogeneous variances.

2.3. Differential gene expression analysis

Differential gene expression analysis was performed with nSolver software using "groups" as the covariate. The Benjamini-Yekutieli method of FDR calculations was selected, and all other analyses were performed with the default settings.

To compare our findings to the related study by Hadjadi et al. we obtained the normalized, log-transformed values from the authors [10]. For differential gene expression, we calculated p-values and FDR values by Student's two-tailed, heteroscedastic t-test, adjusting for false discovery using the Benjamini-Yekutieli method. We maintained COVID-19 severity groups as outlined in the original manuscript [10]. Data and R statistical analysis methods generated by Shen et al. were downloaded from https://github.com/guomics-lab/CVDSBA and run in accordance with the original paper [11].

2.4. Ingenuity Pathway Analysis

Differential gene expression values from the advanced analysis performed by the nSolver software, NanoString Technologies, Inc. were loaded into the Ingenuity Pathway Analysis (IPA) software, Qiagen Digital Insights. Log_2 transformed and Benjamini-Yekutieli calculated FDR values were used as input for further analyses. The "Antigen Presentation Pathway" in IPA (Figure 3A) was loaded and expanded using the grow function. All upstream regulators of CIITA and PAX5 were loaded onto the pathway. Only transcripts that were represented within the dataset were selected, all others were removed. As CD19 is a known target of PAX5 in B cell signaling and lineage maintenance, it was included in the final pathway. The "Complement System" pathway was left unmodified.

2.5. Cell-type analysis

Cell-type analysis and scoring in nSolver software was performed for each of the covariate groups. A significant correlation between immune cell type-specific gene set expression over all samples was used to determine the validity of the cell-type score, indicating the relative abundance of a given cell type. A significant correlation between CD8A and CD8B was used to estimate the abundance of $CD8^+$ T cells ($p = 0.01$), and the B cell population was estimated using a correlation between CD19 and Membrane Spanning 4-Domains A1 (MS4A1) ($p = 0$). Cell-type scores were then log2 transformed, and gaussian statistical analysis t-tests were performed with homogeneous variances.

3. Results

3.1. COVID-19 increased SERPING1 and its encoded protein, C1 esterase inhibitor–central to coagulation and complement regulation.

A visual inspection of the hierarchical analysis in Ong et al., where relative gene expression values were clustered by function for 10 healthy

controls and 22 COVID-19 samples collected from 3 patients, showed roughly three distinct phases of gene expression in case 1, two phases in case 2, and relatively stable gene expression throughout the more limited temporal samples of case 3 [8].

To justify our statistical analysis, we took an unbiased approach to assign the clinical samples into groups and performed an unsupervised hierarchical clustering analysis (HCA) of all 32 clinical samples by similarities in global gene expression profiles (Figure 1A). Visually, the left 15 columns showed increased global immune transcript expression (higher proportion of yellow) compared to the other 17 columns (higher proportion of blue).

All healthy control (HC) samples clustered together two branch points down, and, surprisingly, group 1 (case 1 days (d)4–6) co-clustered with the HC group off of the first branch point away from all of the other case samples, implying that despite all other factors (relation, time of illness, etc.), the unweighted global immune profile during these days of infection of case 1 was more closely related to the HC group than the other COVID-19 samples. Group 1 displayed the most severe clinical symptoms of COVID-19 during this phase, with SO_2 nadir on day 5. As expected, group 1 displayed a global increase in immune response-related transcripts, but, unexpectedly, this was the only cluster that had higher unweighted global gene expression levels of immune-response related transcripts than HC samples. For a statistical comparison of the differential gene expression observed in Group 1 compared to all other groups, see Table S6.

The rest of the clinical samples clustered together on a separate tree, with group 2 (case 2 d6 and d7) clustering the closest to the tree with group 1 and HC. The clinical course of case 2 was characterized by mild symptoms without the presence of a fever, so it may be expected that samples from this case would cluster closer to the HC group. Sharing a node two levels down with group 2 are group 3 (case 2 d8-10) and group X

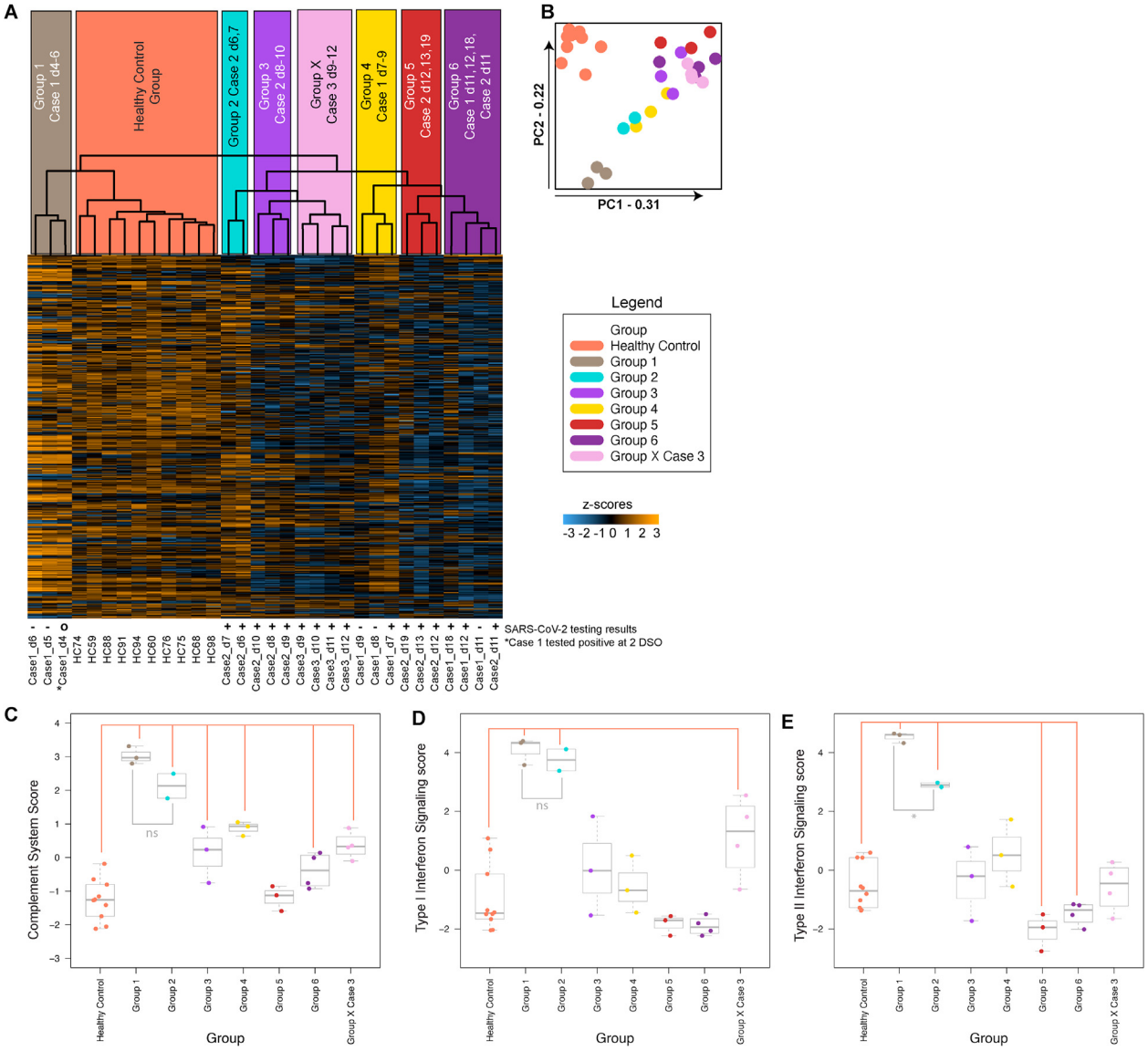

Figure 1. COVID-19 increased complement scores and elicited interferon type-I signaling response regardless of symptom severity. (A) Hierarchical clustering analysis dendrogram showing eight clusters over 32 samples that were used to form groups for further analysis. Orange indicates expression higher than the mean, and blue indicates expression lower than the mean. (B) Principal component (PC) analysis showing that groups defined based on unsupervised hierarchical clustering also associated with each other over PC1 and PC2. PC1 and PC2 contributed to 31% and 22%, respectively, of the variability in these data. (C–E) Boxplot graphs of samples showing the mean and variance of pathway scores plotted against each group defined in (A); salmon-colored bars indicate scores that are significantly different from HC ($p < 0.05$); grey-colored bars report non-significance (ns) or significantly different (*) scores between Group 1 and 2, ($p < 0.05$); for more comparisons, see Table S9 (C) Complement system scores showing significantly more positive scores compared to HC in groups 1–4, 6, and X. (D) IFN-I signaling pathway scores were significantly more positive in groups 1, 2, and X compared to HC. (E) Type II pathway scores were significantly more positive in groups 1, 2, 5, 6, and X compared to HC.

(all samples from case 3). The clustering of groups 3 and X implies that despite the genetic differences between these unrelated cases, the course of the viral infection was most similar between mild case 2 and mild-moderate case 3, many days after the onset of COVID-19 symptoms.

In a separate sub-cluster, group 4 (case 1 d7-9) shares a second-down branch point with group 5 (case 2 d12, d13, and d19) and group 6 (case 1 d11, d12, and d18 and case 2 d11). The distant separation of clusters corresponding to group 1 (case 1 d4-6) and group 4 (case 1 d7-9) may be due to either the effects of the antiviral medication or the natural course of infection, despite their temporal nature. It appears that the final phase of infection for both clinically distinct cases 1 and 2 begins on day 11, at which time both case 1 and case 2 d11 converge into one closely related cluster.

Principal component (PC) analysis grouped each sample by the strength of similarity and showed that groups defined based on hierarchical clustering also associated with each other over PC1 and PC2, which represented 31% and 22% of the variation between samples, respectively (Figure 1B). Based on the expression of genes captured by the first principal component (PC1 – x-axis), group 1 closely associated with HC samples and was positioned between HC and the rest of the COVID-19 samples, unlike in the hierarchal clustering analysis. When similarities were weighted along the second component that contributed the second-highest level of variance in gene expression between samples (PC2 – y-axis), the group 1 cluster showed the highest degree of separation from HC and group 5, which corresponds temporally to the latest samples collected from case 2 (d12–13, d19). See Table S7 for the PC loadings for all transcripts over PC1-6.

Group 1 (case 1 d4-6) represented the earliest samples collected from the most severe patient, and thus we selected for further analysis differentially expressed transcripts based on the significance of differential expression between HC and group 1 ($p < 0.01$). The top 20 differentially increased and decreased transcripts in group 1 represented diverse genes encompassing several facets of innate, adaptive, and other related immune responses (S1 Table). The topmost differentially increased gene in group 1 was also significantly increased in groups 2 and X, and thus all three cases during their clinical courses experienced an increased abundance of serine protease inhibitor (serpin) family G, member 1 (SERPING1). SERPING1 is transcriptionally regulated by IFN-gamma (IFNG) activation of STAT-1 [12], and Cameron et al. showed that SERPING1 transcripts were increased in whole blood mRNA sampled from SARS-CoV-1 patients [9]. Further, Hadjadj et al. reported a significant increase SERPING1 when comparing whole blood mRNA collected from 11 COVID-19 patients to 13 HC [10]. Differences were not reported for comparisons between severe and critical patients compared to HC samples; thus, we performed an independent analysis and observed a significant increase in SERPING1 abundance in all three COVID-19 severity groups, mild/moderate, severe, and critical, compared to HC (log_2 fold-ratio COVID-19 vs healthy controls, FDR<0.01; mild/moderate: 5.30-fold; severe: 5.33-fold; critical: 4.81-fold).

SERPING1 RNA levels do not always mirror the abundance of C1 esterase inhibitor (C1–INH), the protein encoded by SERPING1 [13]. Shen et al. characterized proteins in COVID-19 patient sera and identified C1–INH as 1 of 29 important distinguishing proteins and metabolites increased in sera from patients with severe compared to non-severe COVID-19 [11]. C1–INH was significantly increased in non-severe COVID-19 patients when compared to healthy controls [11].

In addition to C1–INH, Shen et al. also reported the involvement of complement proteins and metabolites in COVID-19 patients [11]. Complement-associated transcripts significantly increased more than two-fold in our dataset, resulting in both a significantly increased complement pathway score for groups 1–4, 6, and X compared to HC and increases in components of the canonical IPA pathway "Complement System" (S2 Table, Figures 1C and 2A, C). We found a notable overlap

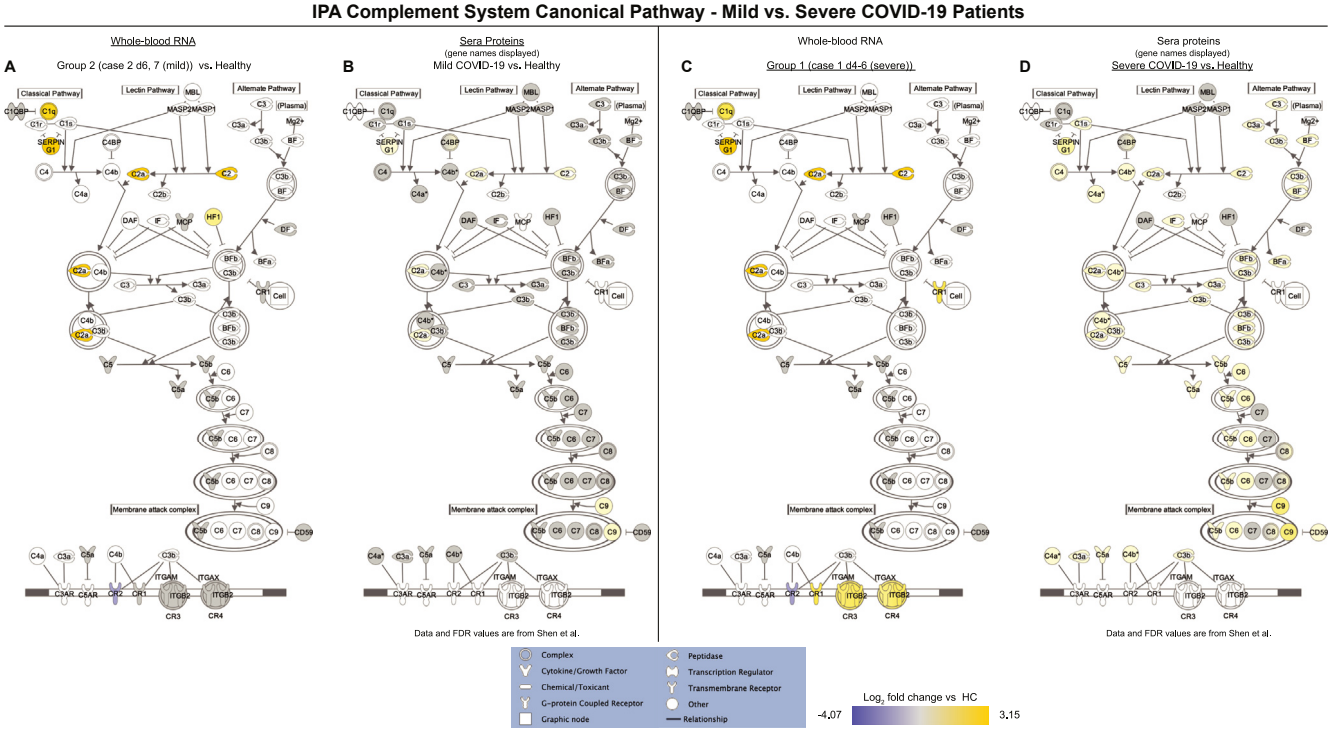

Figure 2. COVID-19 increased SERPING1 and the encoded protein, C1 esterase inhibitor, a central regulator of coagulation and complement regulation, regardless of symptom severity. (A–D) Ingenuity Pathway Analysis (IPA) "Complement System" canonical pathway; yellow and blue fill denotes significantly (FDR<0.01) increased or decreased log_2 fold-regulation over HC, respectively. (A and C) Overlaid differential expression (DE) values of RNA when compared to HC for groups 2 and 1, respectively. Grayed molecules are in the dataset but do not meet the cutoff of more than 2-fold regulated with FDR<0.01. (B and D) Overlaid serum protein values for patients with non-severe and severe COVID-19, respectively, compared to healthy controls. Values and FDR calculations were performed as in Shen et al. [11]. The corresponding gene names are displayed, although these data represent differentially abundant serum proteins. Grayed molecules are in the dataset but do not meet the cutoff of FDR<0.01. The key to each gene name can be found in the S5 Table.

between increased transcripts in cases 1 and 2 when we superimposed COVID-19 serum protein levels that were differentially abundant compared to healthy controls (FDR<0.01) [11] onto the IPA complement system pathway (Figure 2B, D).

3.2. COVID-19 elicited interferon type-I signaling responses regardless of symptom severity.

Consistent with positive complement system scores, more than 50% of IFN type I (IFN–I)- and IFN-II-related transcripts increased, resulting in significantly positive pathway scores (S3 Table and Figure 1D, E). IFN signaling effectively controls viral infection; however, viruses have evolved defense mechanisms to evade IFN-mediated viral clearance [14]. In bronchoalveolar lavage fluid from COVID-19 patients, ISGs were strongly increased, implying a robust IFN response [15]. Both IFN-I and –II pathway scores were significantly increased compared to HC in groups 1 (severe) and 2 (mild) (Figure 1D, E). IFN responses between groups 1 and 2 were strikingly similar, with 13 shared transcripts more than two-fold increased. Furthermore, IFN-induced transmembrane family member 1 (IFITM-1), IFN induced protein 35 (IFI35), and C-X-C motif chemokine ligand 10 (CXCL10), all ISGs, were differentially increased in both groups 1 and 2. These data imply that although afebrile with a mild cough and sore throat, case 2 experienced a significant IFN response to SARS-CoV-2 infection. Consistently, Hadjadj et al. observed robust IFN-I and IFN-II responses in mild/moderate COVID-19 patients [10].

Although upregulated by IFN-γ, MHC class II receptors (HLA-DMB/OB/PB1/RA/RB1/RB3) and the MHC class II upstream transcriptional regulator CIITA were strongly decreased compared to HC in group 1 (early, severe), and at least one HLA gene was significantly decreased in all groups (S4 Table). The decrease in CIITA in group 1 was observed despite increases in several upstream inducers (PML, IRF1, BCL6, STAT 1–3); however, this increase was not seen in the upstream inducer PAX5 (Figure 3B). PAX5 is a signature B cell gene that is required for B cell lineage commitment, lineage restriction, and maturation [16, 17], and inhibition of PAX5 transcription reduces its target gene, CD19, and re-programs mature B cells into macrophages [18]. Although not observed in Hadjadj et al. [10], both PAX5 and CD19 were significantly decreased in all of the COVID-19 sample groups, regardless of genetic background or clinical severity, and levels had not recovered by 18 or 19 DSO in cases 1 and 2 (group 5 (case 2 d12, d13, d19) and group 6 (case 1 d11, d12, d18 and case 2 d11)) (Figure 3C–H).

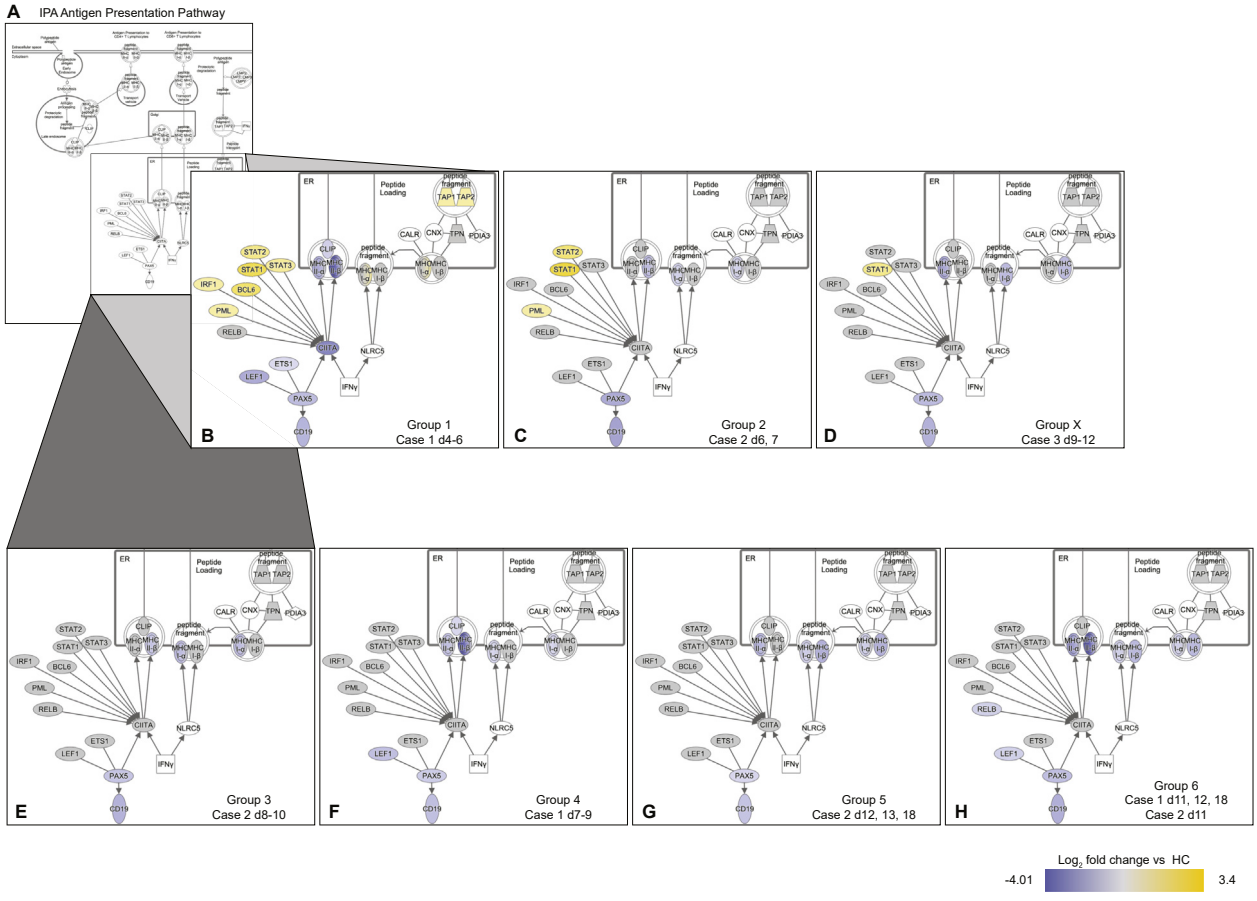

Figure 3. COVID-19 reduced B cell signature, specification, and lineage commitment gene abundance regardless of symptom severity. (A) Ingenuity Pathway Analysis (IPA) "Antigen Presentation Pathway" showing MHC-I and II antigen presentation pathways with the addition of genes represented in the data set which are also 1) upstream regulators of CIITA (STAT 1–3, BCL6, IRF1, PML, RELB, and PAX5), 2) upstream regulators of PAX5 (LEF1 and ETS1) and 3) a downstream target of PAX5 (CD19). (B–H) Zoomed square in (A) to show detail. Overlaid are Log_2 fold-change differential expression (DE) values when compared to HC for each covariate group. All groups showed increases in STAT1 and decreases in PAX5, and CD19. Yellow and blue fill denote significantly (FDR<0.01) increased or decreased fold-regulation over HC, respectively. (B) In addition to DE in all groups, group 1 (case 1 d4-6 (severe)) showed increases in MHC-I signaling components, HLA-A, TAP1/2. Despite increased upstream regulators (STAT 1–3, BCL6, IRF1, PML), CIITA was not increased. MHC-II receptors (HLA-DMA/B/OB/PB1/RA/RB1/RB3), CLIP (CD74), LET1, and ETS1showed decreased DE. (C) Group 2 (case 2 d6, 7 (mild)) showed increased HLA-C, STAT1/2, and PML and decreases in HLA-DOB/RB. (D) Group X (Case 3 (d9-12 mild-moderate)) displayed decreased HLA-DRA abundance. (E) Group 3 showed decreased HLA-C, and HLA-DOB/RB1. (F) Group 4 showed decreased CLIP (CD74), LEF1, HLA-C, and HLA-DMB/OB/PB1/RA/RB1/DRB3. (G) The latest clinical samples for case 2 (mild) d12, 13, and 18 (group 5) showed decreased HLA-C and HLA-DOB/RA/RB1. (H) The latest clinical samples for case 1 (severe) (group 6) showed decreased RELB, LEF1, HLA-C and HLA-DMB/OB/PA1/DPB1/RA/RB1. Greyed molecules are in the dataset but do not meet the cutoff of more than 2-fold regulated with an FDR<0.01.

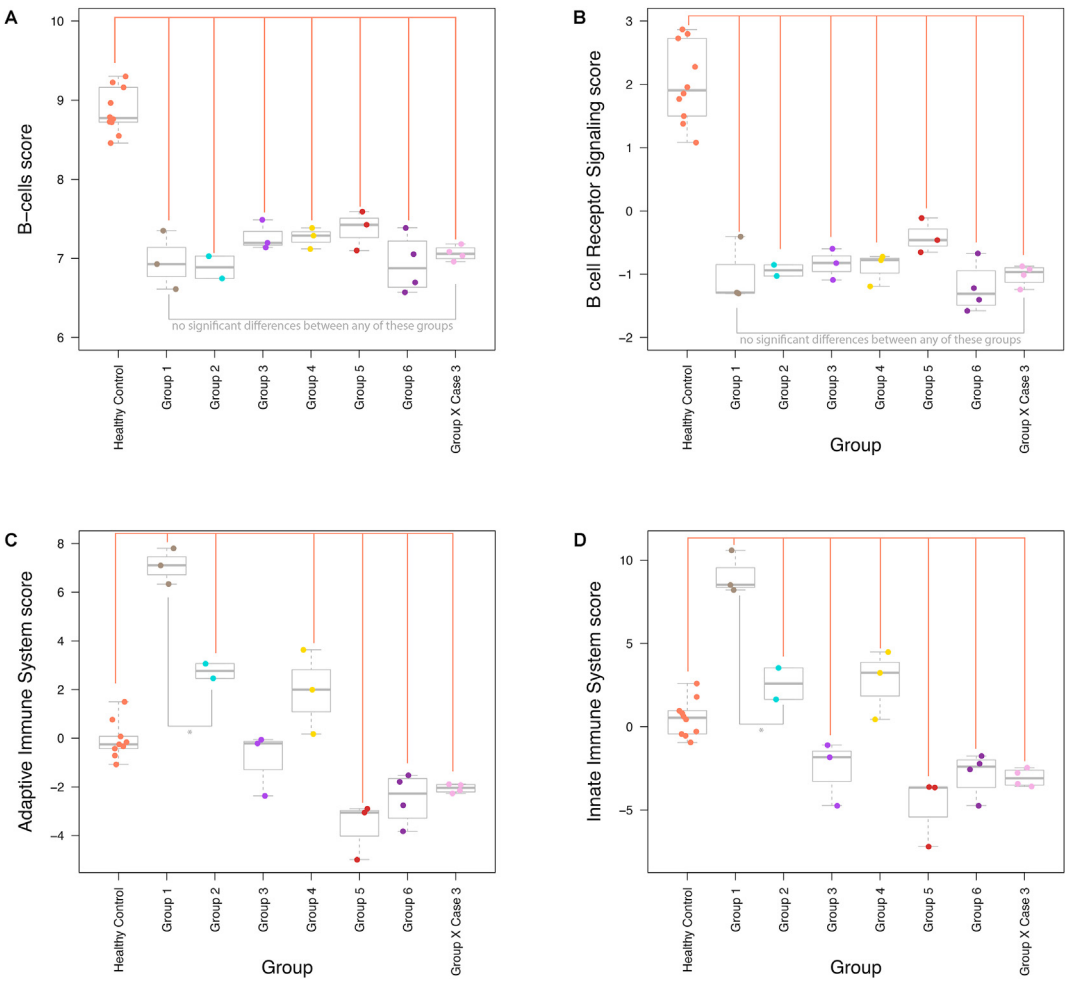

Figure 4. COVID-19 negatively affected estimated B cell abundance, and globally depressed adaptive and innate immune-related transcripts as SARS-CoV-2 infection resolved. (A–E) Boxplot graphs of means and variance of cell scores (A and B) or pathway scores (C–E) plotted against each group; salmon-colored bars indicate scores that are significantly different from HC ($p < 0.05$); grey-colored bars report significantly different (*) scores between Group 1 and 2, ($p < 0.05$); for more comparisons, see Table S9 (A) B cell scores imply a significant depletion in the estimated abundance of this cell in all groups when compared to HC. There were no significant differences between group samples. (B) B cell receptor signaling aligns with estimated B cell numbers, which showed as significantly more negative than HC. There were no significant differences between group samples. (D) Although adaptive immune-related transcripts increased in groups 1, 2, and 4, this cohort of genes was significantly depressed later in the clinical course of COVID-19 groups 5, 6, and X. (E) Innate immune-related transcript scores were significantly increased in groups 1, 2, and 4 but were significantly decreased compared to HC in groups 3, 5, 6, and X, representing the later phases of COVID-19 recovery.

3.3. COVID-19 negatively affected estimated B cell abundance, and globally depressed adaptive and innate immune-related transcripts as SARS-CoV-2 infection resolved.

Consistent with the patterns of expression of PAX5 and CD19, there was a striking depletion of estimated numbers of B cells in all COVID-19 groups comprising clinical samples from all three cases, implying that B cell populations were negatively affected regardless of COVID-19 infection severity (Figure 4A). Considering that in the mild COVID-19 case 2 the estimated B cell abundance had not recovered by 19 DSO, it would have been of great clinical interest to have determined whether B cell populations had recovered by 29 DSO. Pathway scores for B cell signaling were negative compared to HC over all groups (Figure 4B). Although increases in adaptive and innate immune system-related transcripts occurred in groups 1 and 2, these gene sets were significantly decreased compared to HC in the later phases of recovery for groups 5, 6, and X, implying global suppression of innate and adaptive immune responses as SARS-CoV-2 infection resolves (Figure 4C, D).

4. Conclusions

Although these data are from a limited number of patients, we observed remarkably parallel immune responses in case 1 and his son, case 2, despite starkly different clinical courses. Case 1 was hospitalized for an extended period and required supplemental oxygen, whereas his son's symptoms were mild, and he was without fever over 29 days of SARS-CoV-2 infection. Under other circumstances, case 2 may have dismissed his mild cough and sore throat as seasonal allergies, a cold, or air-quality issues in the absence of a fever and never realized he was positive for SARS-CoV-2. Currently there is an extreme paucity of information regarding the immune response over the course of infection in individuals that have very mild symptoms, as other related clinical studies have inclusion criteria that include fever or hospitalization [10, 19, 20, 21]. Our study showed that a number of diverse immune and inflammatory pathways were activated or repressed in afebrile case 2.

All three cases showed signs of global immune depression, and we speculate that a potential dramatic increase of SERPING1-encoded

C1–INH may be viewed as a biological feedback response to contact and complement hyperactivation and hypercoagulability associated with COVID-19.

SARS-CoV-2 infection may be associated with hypercoagulopathy, and this possibility has become one of the major focuses of COVID-19 research [1, 2, 3, 4, 5, 6]. C1–INH suppresses activation of complement, coagulation, inflammation, and fibrinolysis through inhibition of the contact system [22]. This system is termed the contact system because the serine protease, factor XII (FXII) is activated by contact with anionic surfaces resulting in 1) the activation of the Kallikrein-Kinin pathway that drives bradykinin-associated inflammation, 2) cleavage of FXI, resulting in increased thrombin, fibrin formation, and fibrin clot formation, 3) activation of complement through C1r and C1s, and 4) promotion of fibrinolysis [22].

C1–INH is the primary inhibitor of FXIIa in the plasma and is the only known natural inhibitor of the classical complement proteins C1r and C1s, such that they are unable to form the C1 complement activating complex [23, 24]. Further C1–INH inhibits the other two complement activation pathways by binding to maltose-binding lectin (MBL)-associated serine protease (MASP)-1 and -2 and C3b, activators of the lectin and alternative complement pathways, respectively. Deposition of complement proteins on the surface of SARS-CoV-1 has been shown to inhibit infection *in vitro* [25] as complement activation is a first line of defense against viral infection [26].

SERPING1 is an IFN-stimulated gene (ISG) and acts in a negative-feedback loop to control contact and complement system activation to avoid damage to healthy host cells [27]. CR1, CR3, and CR4 complexes inhibit complement activation, and components of these complexes were differentially increased in group 1 (S2 Table). Increased differential expression of complement-activating proteins C2 and C1QB [27] between HC and groups 1–3 and X implies complement activation. Notably, in the mild and moderate cases 2 and X, complement inhibitor transcripts were either not regulated or decreased (S2 Table). Significantly increased complement proteins and members of the membrane attack complex support the idea that complement is hyperactivated COVID-19 patients [11].

In SARS-CoV-2 patients, increased SERPING1-encoded C1–INH may be interpreted as an attempt by the host to inhibit inappropriate complement activation. Activated complement-associated microvascular injury by fibrin deposition and neutrophil permeation has been observed in severe COVID-19 patients that experienced respiratory failure and purpuric skin rashes [2]. A recent pre-print showed that *in vitro* C1–INH attenuates SARS-CoV-2 nucleocapsid protein-mediated complement activation [28], and treatment of COVID-19 patients with complement inhibitors may be a viable therapeutic option [28, 29, 30]. Recent clinical data showed promising results when severe COVID-19 patients were administered recombinant C1–INH [31, 32]. Nonetheless, considering that C1–INH acts to broadly suppress innate and adaptive immune responses, caution must be considered prior to implementing widespread use C1–INH in COVID-19 patients [25, 27]. Further, interrogation of data from Overmyer et al. using the online resource, covid-omics.app, shows that there is a significant association between increased SERPING1 and C1–INH in COVID-19 hospitalized patients versus non-COVID-19 hospitalized patients (see Table S10 for more information) [20], and thus, further increases in C1–INH may have detrimental effects.

It is tempting to speculate that mild case 2 may have had an extended viral load because of an insufficient humoral immune response due to the immunosuppressive actions of increased C1–INH. If C1–INH is also increased in asymptomatic patients it may be a contributing factor to the observed prolonged SARS-CoV-2 viral load and decreased levels of viral specific IgG versus those that were symptomatic [33]. Identifying truly asymptomatic versus pre-symptomatic versus mild COVID-19 patients is a complex process as has been outlined in Long et al. [33]. Execution of such a clinical study is currently outside our focus of treating severe COVID-19 patients within our facilities. We think that our study provides important insight into patients that may otherwise go untested and uncharacterized due to the benign nature of their symptoms. Our purpose is to bring forth these data to the scientific community and spur ongoing studies of SARS-CoV-2 infected individuals with little to no COVID-19 symptoms.

To our knowledge, we are the first to propose a connection between SERPING1-encoded C1–INH, complement activation, and hypercoagulation, in asymptomatic or patients with very mild COVID-19 symptoms. A hyper-response to aberrant complement activation by the extreme upregulation of SERPING1-encoded C1–INH may lead to widespread immunodepression, similar to what is observed in patients with systemic inflammatory syndrome [34]. Consideration must be given to the long-term effects, such as decreased humoral immunity, of the dysregulation of these pathways in COVID-19 patients, especially those with potentiating comorbidities that may contribute to higher re-infection risk.

Declarations

Author contribution statement

Melissa A. Hausburg: Conceived and designed the experiments; Performed the experiments; Analyzed and interpreted the data; Wrote the paper.

Kaysie L. Banton, Michael Roshon: Analyzed and interpreted the data.

David Bar-Or: Conceived and designed the experiments; Analyzed and interpreted the data; Wrote the paper.

Funding statement

This research did not receive any specific grant from funding agencies in the public, commercial, or not-for-profit sectors.

Data availability statement

Data associated with this study has been deposited at Mendeley under https://doi.org/10.17632/sbv5rnmp8t.1, https://data.mendeley.com/datasets/sbv5rnmp8t/draft?a=d8bedf37-2782-49b9-aea6-e8589503057b.

Declaration of interests statement

The authors declare no conflict of interest.

Additional information

Supplementary content related to this article has been published online at https://doi.org/10.1016/j.heliyon.2020.e05877.

Acknowledgements

The authors would like to thank Rick Calvo for his input into the hierarchical clustering and principal component analyses used in this study and Erica Sercy for proofreading and editing of the manuscript.

References

[1] N. Vabret, G.J. Britton, C. Gruber, S. Hegde, J. Kim, M. Kuksin, et al., Immunology of COVID-19: current state of the science, Immunity 52 (6) (2020) 910–941.

[2] C. Magro, J.J. Mulvey, D. Berlin, G. Nuovo, S. Salvatore, J. Harp, et al., Complement associated microvascular injury and thrombosis in the pathogenesis of severe COVID-19 infection: a report of five cases, Transl. Res. 220 (2020) 1–13.

[3] S. Cui, S. Chen, X. Li, S. Liu, F. Wang, Prevalence of venous thromboembolism in patients with severe novel coronavirus pneumonia, J. Thromb. Haemostasis 18 (6) (2020) 1421–1424.

[4] N. Tang, D. Li, X. Wang, Z. Sun, Abnormal coagulation parameters are associated with poor prognosis in patients with novel coronavirus pneumonia, J. Thromb. Haemostasis 18 (4) (2020) 844–847.

[5] S. Yin, M. Huang, D. Li, N. Tang, Difference of coagulation features between severe pneumonia induced by SARS-CoV2 and non-SARS-CoV2, J. Thromb. Thrombolysis (2020).
[6] M. Panigada, N. Bottino, P. Tagliabue, G. Grasselli, C. Novembrino, V. Chantarangkul, et al., Hypercoagulability of COVID-19 patients in intensive care unit: a report of thromboelastography findings and other parameters of hemostasis, J. Thromb. Haemostasis 18 (7) (2020) 1738–1742.
[7] N.W. Furukawa, J.T. Brooks, J. Sobel, Evidence supporting transmission of severe acute respiratory syndrome coronavirus 2 while presymptomatic or asymptomatic, Emerg. Infect. Dis. 26 (7) (2020).
[8] E.Z. Ong, Y.F.Z. Chan, W.Y. Leong, N.M.Y. Lee, S. Kalimuddin, S.M. Haja Mohideen, et al., A dynamic immune response shapes COVID-19 progression, Cell Host Microbe 27 (6) (2020) 879–882 e2.
[9] M.J. Cameron, L. Ran, L. Xu, A. Danesh, J.F. Bermejo-Martin, C.M. Cameron, et al., Interferon-mediated immunopathological events are associated with atypical innate and adaptive immune responses in patients with severe acute respiratory syndrome, J. Virol. 81 (16) (2007) 8692–8706.
[10] J. Hadjadj, N. Yatim, L. Barnabei, A. Corneau, J. Boussier, N. Smith, et al., Impaired type I interferon activity and inflammatory responses in severe COVID-19 patients, Science 369 (6504) (2020) 718–724.
[11] B. Shen, X. Yi, Y. Sun, X. Bi, J. Du, C. Zhang, et al., Proteomic and metabolomic characterization of COVID-19 patient sera, Cell 182 (1) (2020) 59–72 e15.
[12] K. Zahedi, A.E. Prada, J.A. Prada, A.E. Davis 3rd, Characterization of the IFN-gamma-responsive element in the 5' flanking region of the C1 inhibitor gene, J. Immunol. 159 (12) (1997) 6091–6096.
[13] R. Lubbers, J.S. Sutherland, D. Goletti, R.A. de Paus, D.J. Dijkstra, C.H.M. van Moorsel, et al., Expression and production of the SERPING1-encoded endogenous complement regulator C1-inhibitor in multiple cohorts of tuberculosis patients, Mol. Immunol. 120 (2020) 187–195.
[14] R.E. Randall, S. Goodbourn, Interferons and viruses: an interplay between induction, signalling, antiviral responses and virus countermeasures, J. Gen. Virol. 89 (Pt 1) (2008) 1–47.
[15] Z. Zhou, L. Ren, L. Zhang, J. Zhong, Y. Xiao, Z. Jia, et al., Heightened innate immune responses in the respiratory tract of COVID-19 patients, Cell Host Microbe 27 (6) (2020) 883–890 e2.
[16] C. Palmer, M. Diehn, A.A. Alizadeh, P.O. Brown, Cell-type specific gene expression profiles of leukocytes in human peripheral blood, BMC Genom. 7 (2006) 115.
[17] C. Cobaleda, A. Schebesta, A. Delogu, M. Busslinger, Pax5: the guardian of B cell identity and function, Nat. Immunol. 8 (5) (2007) 463–470.
[18] H. Xie, M. Ye, R. Feng, T. Graf, Stepwise reprogramming of B cells into macrophages, Cell 117 (5) (2004) 663–676.
[19] A. D'Alessandro, T. Thomas, M. Dzieciatkowska, R.C. Hill, R.O. Francis, K.E. Hudson, et al., Serum proteomics in COVID-19 patients: altered coagulation and complement status as a function of IL-6 level, J. Proteome Res. (2020).
[20] K.A. Overmyer, E. Shishkova, I.J. Miller, J. Balnis, M.N. Bernstein, T.M. Peters-Clarke, et al., Large-scale multi-omic analysis of COVID-19 severity, Cell Syst. (2020).
[21] C. Lucas, P. Wong, J. Klein, T.B.R. Castro, J. Silva, M. Sundaram, et al., Longitudinal analyses reveal immunological misfiring in severe COVID-19, Nature 584 (7821) (2020) 463–469.
[22] A.T. Long, E. Kenne, R. Jung, T.A. Fuchs, T. Renne, Contact system revisited: an interface between inflammation, coagulation, and innate immunity, J. Thromb. Haemostasis 14 (3) (2016) 427–437.
[23] A.E. Davis 3rd., Structure and function of C1 inhibitor, Behring Inst. Mitt. (84) (1989) 142–150.
[24] A.E. Davis 3rd, P. Mejia, F. Lu, Biological activities of C1 inhibitor, Mol. Immunol. 45 (16) (2008) 4057–4063.
[25] P. Agrawal, R. Nawadkar, H. Ojha, J. Kumar, A. Sahu, Complement evasion strategies of viruses: an overview, Front. Microbiol. 8 (2017) 1117.
[26] W.K. Ip, K.H. Chan, H.K. Law, G.H. Tso, E.K. Kong, W.H. Wong, et al., Mannose-binding lectin in severe acute respiratory syndrome coronavirus infection, J. Infect. Dis. 191 (10) (2005) 1697–1704.
[27] J.R. Dunkelberger, W.C. Song, Complement and its role in innate and adaptive immune responses, Cell Res. 20 (1) (2010) 34–50.
[28] T. Gao, M. Hu, X. Zhang, H. Li, L. Zhu, H. Liu, et al., Highly pathogenic coronavirus N protein aggravates lung injury by MASP-2- mediated complement over-activation, MedRxiv (2020).
[29] P.F. Stahel, S.R. Barnum, Complement inhibition in coronavirus disease (COVID)-19: a neglected therapeutic option, Front. Immunol. 11 (2020) 1661.
[30] A.M. Risitano, D.C. Mastellos, M. Huber-Lang, D. Yancopoulou, C. Garlanda, F. Ciceri, et al., Complement as a target in COVID-19? Nat. Rev. Immunol. 20 (6) (2020) 343–344.
[31] Conestat alfa in the prevention of severe SARS-CoV-2 infection in hospitalized patients with COVID-19 [Interventional (Clinical Trial)]. Available from: https://clinicaltrials.gov/ct2/show/NCT04414631, 2020.
[32] P. Urwyler, S. Moser, P. Charitos, I. Heijnen, M. Rudin, G. Sommer, et al., Treatment of COVID-19 with conestat alfa, a regulator of the complement, contact activation and Kallikrein-Kinin system, Front. Immunol. 11 (2020) 2072.
[33] Q.X. Long, X.J. Tang, Q.L. Shi, Q. Li, H.J. Deng, J. Yuan, et al., Clinical and immunological assessment of asymptomatic SARS-CoV-2 infections, Nat. Med. 26 (8) (2020) 1200–1204.
[34] C.P. Cabrera, J. Manson, J.M. Shepherd, H.D. Torrance, D. Watson, M.P. Longhi, et al., Signatures of inflammation and impending multiple organ dysfunction in the hyperacute phase of trauma: a prospective cohort study, PLoS Med. 14 (7) (2017), e1002352.